J. Membrane Biol. 137, 237–247 (1994)

The Journal of
Membrane
Biology

Cl^- Currents of Unstimulated T84 Intestinal Epithelial Cells Studied by Intracellular Recording

M.A. Valverde, G.M. Mintenig*, F.V. Sepúlveda
AFRC Babraham Institute, Babraham Hall, Cambridge CB2 4AT, United Kingdom

Received: 12 July 1993/Revised: 6 October 1993

Abstract. The ionic currents spontaneously present in T84 intestinal epithelial cells, a line of colonic carcinoma origin, have been studied using the whole-cell recording mode of the patch-clamp technique and the single-electrode voltage-clamp method. Patch-clamp experiments showed that nonstimulated T84 cells already possess large currents but that these tend to disappear during the course of the experiments, presumably through the dialysis of some essential cytoplasmic component against the micropipette solution. The main charge carrier in these experiments appears to be Cl^- as judged from ion replacement. Microelectrode impalement of T84 cells gave a membrane potential of around −30 mV, similar to the equilibrium potential for Cl^- estimated from previously published values for intracellular Cl^- concentration. Voltage-clamp experiments with a single microelectrode revealed three kinetically distinguishable current patterns; currents decaying during hyperpolarizing voltage pulses, currents slowly activating during hyperpolarizing pulses and time-independent currents. The appearance of these distinct kinetic patterns was not predictable from cell to cell, and was not dependent on extracellular Ca^{2+}. Ionic replacement experiments suggest that the charge carrier was always Cl^-, regardless of the kinetic pattern observed. No K^+ currents appear to be present in the nonstimulated T84 cells. Exposure of T84 cells to the muscarinic agonist carbachol induced a shift in the membrane potential towards more negative values, consistent with an activation of a K^+ conductance. Thus, we suggest that the resting membrane potential in T84 cells is determined by the distribution of Cl^-. This might imply that activation of K^+ conductance could by itself support secretion by T84 monolayers through tonically active Cl^- channels.

Key words: Chloride currents — Single electrode voltage clamp — Chloride secretion — T84 cells

Introduction

Colonic carcinoma T84 cells are a very useful model of Cl^- secretory epithelium. They respond to secretagogues, such as carbachol, prostaglandin E_1 and vasoactive intestinal peptide (VIP) with Cl^- secretion. This secretion is thought to be mediated by an apical Cl^- conductance through which Cl^- ions exit to the apical bathing solution. Extensive ion transport work (Dharmsathaphorn & Pandol, 1986; Mandel, Dharmsathaphorn & McRoberts, 1986) on T84 cells grown to form confluent monolayers has shown that essentially no transepithelial net transfer of ions occurs unless cells are stimulated. Stimulation of receptors that activate cAMP production, such as VIP receptors, appears to increase the apical Cl^- conductance and a basolateral K^+ conductance which, by causing hyperpolarization, contributes to maintaining an electrochemical potential gradient favorable to Cl^- exit. Muscarinic receptor activation, on the other hand, increases secretion only transiently. This has been shown to occur through transient activation of K^+ channels that would generate the driving force for Cl^- exit via a tonically active Cl^- conductance. These results, which were obtained by measuring transepithelial or cellular radioisotopic fluxes, would suggest that sustained secretion depends on the activation of both Cl^- and K^+ channels. K^+-chan-

* *Present address:* Department de Ciències Médiques Basiques, Facultat de Medicina, E-25006, Lleida, Spain

Correspondence to: M.A. Valverde

nel activation by itself, however, seems to be able to induce some Cl^- secretion through what would appear to be Cl^- channels active in the resting state. This suggests that Cl^- channels have some activity at rest and that Cl^- is at or near equilibrium when no stimulation is present. Studies using the whole-cell recording mode of the patch-clamp technique have shown that T84 cells have negligibly low currents of any kind, Cl^- and K^+ currents appearing only after stimulation (Cliff & Frizzell, 1990; Devor, Simasko & Duffey, 1990). However, evidence for a basal Cl^- conductance in unstimulated T84 cells has been reported (Devor et al., 1990). This apparent discrepancy prompted us to investigate further the membrane current systems present in unstimulated T84 cells.

In the present series of experiments, we use the whole-cell recording patch-clamp approach to show that Cl^- currents are indeed present and that they dominate the membrane conductance of unstimulated T84 cells. They are, however, rapidly attenuated, presumably through dialysis of some essential cytoplasmic component. Experiments using the single intracellular microelectrode voltage-clamp technique (SEVC), which allows measurements without intracellular dialysis, show these currents to remain stable even for prolonged periods. It is then possible to demonstrate that the selectivity of the membrane of unstimulated T84 cells is dominated by Cl^- conductance. Marked differences in kinetics are found between cells, which suggest that three different types of channels selective to Cl^- might be present in T84 cells. A preliminary communication of these data has been presented to the Physiological Society (Valverde et al., 1991*a*).

Materials and Methods

Cell Culture

T84 cells were grown in 1:1 mixture of Dulbecco's modified Eagle's medium (DMEM) and Ham's F-12 supplemented with 2 mM HEPES, 10% fetal calf serum, 80 IU/ml penicillin, 8 mg/ml streptomycin. Cells were incubated at 37°C in a humidified atmosphere of 5% CO_2 in air. For electrophysiological experiments, cells were seeded onto glass coverslips or 35 mm diameter cell culture plastic petri dishes, and used 1–3 days after subculturing by which time they had not reached confluence.

Electrophysiological Recordings

Standard whole-cell patch-clamp or single microelectrode voltage-clamp recordings were used (Sheppard et al., 1991; Valverde et al., 1991*b*). Coverslips containing the cells were put into a Plexiglass chamber mounted on the stage of an inverted microscope. Alternatively, petri dishes were directly mounted on the microscope stage. Hanks solution (*see* Table 1 for composition) was used to superfuse continuously the cells by gravity and a peristaltic pump was used to remove fluid so that volume was kept constant. Changes in solution were achieved by directing a small jet of the desired solution to the cell under study by means of a device similar to that described by Suzuki, Tachibana and Kaneko (1990). All measurements were carried out at room temperature.

Patch-clamp pipettes were made from thin borosilicate (hard) glass capillary tubing with outside diameter 1.5 mm (Clark Electromedical, Reading, UK), using a two-stage vertical pipette puller (PP-83 Narishige, Japan). Fire-polished pipettes had a resistance of 2–5 MΩ when filled with any of the pipette solutions given in Table 1. Standard patch-clamp whole-cell recordings were made using a List EPC-7 amplifier (List Medical, Germany).

For single electrode voltage-clamp experiments, microelectrodes were made with similar glass as for patch pipettes, but with internal filament (Clark Electromedical), using a two-stage horizontal puller (Narishige PN-3). To decrease capacitance fluctuations due to possible changes in solution level, electrodes were coated externally with a silicone resin (Dow Corning 1-2577 conformal coating). Microelectrodes filled with 150 mM KCl had a tip resistance of 40–70 MΩ when measured in Hanks solution. The microelectrode was connected to the headstage of a high impedance amplifier (Axoclamp 2A, Axon Instruments, Foster City, CA) through an Ag/AgCl wire. A second headstage was used to record bath potential, which was automatically subtracted from the intracellular measurements. Cells were studied using the discontinuous voltage-clamp approach (Wilson & Goldner, 1975; Finkel & Redman, 1984). Sampling frequency was usually 5–15 kHz and the duty cycle was 30% of the period. Other details of the operation were as described elsewhere (Valverde et al., 1991*b*).

Data Acquisition and Analysis

Voltage and current signals from the amplifier, together with synchronizing pulses, were recorded on videotape using a modified digital audio processor (Sony PCM-701ES), or on digital audiotape using a modified DAT recorder (Sony). The signals were digitized using an IBM PC-AT or a Beltron Turbo-AT computer equipped with Cambridge Electronic Design 1401 Laboratory interfaces. Sampling rate was 700 Hz unless otherwise stated. The voltage pulse generator and voltage-clamp analysis programs were written by J. Dempster (University of Strathclyde, Glasgow, Scotland).

Results

Membrane Currents of T84 Cells Measured by the Patch-Clamp Approach

Whole-cell current recordings of unstimulated T84 cells performed with pipette solutions rich in KCl (pipette A) and extracellular solution of normal composition (Hanks) gave zero-current voltages between −30 and −17 mV immediately after breaking into the whole-cell configuration and generally decayed to between −10 and 0 mV within 2–4 min. The initial figures provide an upper limit for E_m, as we cannot be certain of whether any equilibration of pipette solution and cytoplasm had taken place before the current-clamp measurements were taken. Voltage-clamp experiments were performed holding the cell at −40 mV and stepping the

Table 1. Composition of bathing solutions

	Hanks	0Cl(gluconate)	8Cl(glutamate)	8Cl(gluconate)	0Cl/K	Pipette A	Pipette B
KCl	5		5	5		140	
NaCl	140						
$NaHCO_3$	4.2	4.2	4.2	4.2	4.2		
$CaCl_2$	1.3		1.3			0.97	0.1
$MgCl_2$	0.5		0.5			1	1.2
Glucose	5.5	5.5	5.5	5.5	5.5		
HEPES	10	10	10	10	10	10	10
CaGluconate		10		10	10		
KGluconate		5		5	45		
NaGluconate		140		140	100		
MgGluconate		0.5		0.5	0.5		
NaGlutamate			140				
NMDG-Cl							140
EGTA						1	1

All solutions titrated to pH 7.2 with Tris. Concentrations in mM. Pipette solutions always contain 2 mM Na_2ATP and 0.5 mM Na_2GTP. The calculated Ca^{2+} free concentration in pipette solution A was 130 nM and in B < 5 nM. EGTA: ethylglycol-bis (β-aminoethylether) acid.

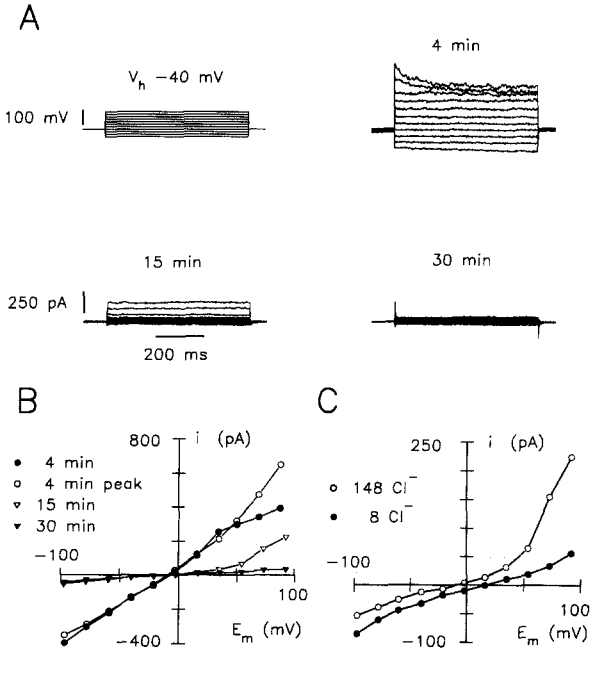

Fig. 1. Attenuation of currents during patch-clamp whole-cell recording in a T84 cell. (*A*) Currents elicited by the voltage protocol shown were recorded 4, 15 and 30 min after breaking into the whole-cell configuration. The composition of the pipette solution is given in Table 1 (pipette A) and the bath solution was Hanks. The holding potential (V_h) is given. (*B*) Current-voltage relation for the traces shown in *A*. For the traces at 4 min, measurements were taken both at the initial peak and at the steady-state. (*C*) Effect of extracellular Cl^- replacement on the currents of T84 cells. The values shown are steady-state measurements taken from a cell bathed in standard extracellular medium (148 Cl^-) and after replacement of all but 8 mM Cl^- by glutamate; experiments done 15 min after breaking into the whole-cell configuration.

voltage from −100 to 100 mV. Figure 1*A* shows families of currents elicited in a cell by the voltage protocol shown, 4, 15 or 30 min after starting the whole-cell recording. Pulses between −100 and 60 mV produced currents that were largely time independent. At 4 min, currents evoked by the more depolarized potentials decayed during the 600 msec pulse. As shown in the current-voltage relation in Fig. 1*B*, peak currents showed slight outward rectification while steady-state currents tended to level off at the most depolarized pulses. A decline in the currents was apparent with decreases of about 60% at 15 min and 95% at 30 min after the start of the recording. The corresponding current-voltage relations are shown in Fig. 1*B*. The decrease in currents was not due to nonspecific damage as cells showing negligible currents could be stimulated with 100 μM carbachol to produce large K^+ currents 20–30 min after breaking into the whole-cell mode (*results not shown*). A similar result has been reported before by Devor et al. (1990).

The ionic species involved in the currents of T84 cells was investigated in ion replacement experiments. Figure 1*B* shows a current-voltage relation obtained with a KCl-rich pipette and normal, NaCl-rich bathing solution. Under these conditions, the total cell current rectified outwardly and reversed at −10 mV. This suggests a dominant role for Cl^- conductance in determining E_m, as in our experimental conditions E_{Cl} was −2 mV, while E_K and E_{Na} were −87 and 97 mV, respectively. As shown in Fig. 1*C*, replacing all but 8 mM of the extracellular Cl^- with glutamate strongly reduced outward currents and displaced the reversal potential by 27 mV in the positive direction. Assuming that anions are the only charge carriers, a permeability ratio $P_{glutamate}/P_{Cl}$ of 0.3 can be calculated from the

shift in reversal potential. Replacement of Na^+ by K^+ in a bathing medium containing 8 mM Cl^- had little effect.[1] When all but 4 mM Cl^- in the pipette-filling solution was replaced by gluconate, only very small inward currents were observed, the current-voltage relation outwardly rectified very markedly and the reversal potential was −30 mV; in these conditions, replacing all but 4 mM extracellular Cl^- by gluconate moved the reversal potential to 0 mV and strongly reduced outward currents (*results not shown*).

A different type of chloride current was also observed using the whole-cell voltage-clamp technique (Fig. 2). This current, elicited by the voltage protocol shown, presented outward rectification with an increase in the current during the most depolarized potentials (family of currents obtained 2 min 30 sec after breaking into the whole-cell mode). Chloride currents with similar characteristics have been identified as Ca^{2+} dependent, both in these cells and in airway epithelial cells (Cliff & Frizzell, 1990; Anderson & Welsh, 1991). The Ca^{2+} concentration of the pipette solution used for the experiment shown in Fig. 2 was <5 nM (pipette B in Table 1). A decline in the currents with time was observed when using such low Ca^{2+} concentration (*see* families taken at 3 min 30 sec and at 4 min 30 sec; similar results were obtained in three other cells). Using pipette solution with a Ca^{2+} concentration >150 nM prevented the disappearance of these currents ($n = 4$).

The transient nature of the currents recorded made difficult their study by the whole-cell recording mode of the patch-clamp technique. To avoid dialysis of intracellular components, voltage-clamp experiments with intracellular microelectrodes were therefore conducted.

Membrane Currents of T84 Cells Measured by the Single Electrode Voltage-Clamp Approach

Current-Clamp Observations

Several properties recorded in current-clamp from cells bathed in Hanks solution are listed in Table 2. The resting potential of the cells, about −30 mV, was consistent with initial current-clamp measurements described in the previous section and also with calculation of E_{Cl} from published intracellular Cl^- concentrations in T84 cells (Mandel et al., 1986). This value was −35 mV,

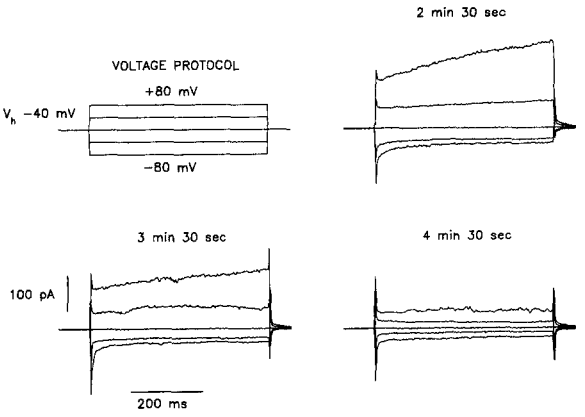

Fig. 2. Time-dependent changes in Cl^- current amplitude after establishing the whole-cell recording mode in a T84 cell. Pipette solution was pipette B and bath solution Hanks (Table 1). Initial currents (2 min 30 sec after breaking into the whole-cell mode), and currents obtained at 3 min 30 sec and 4 min 30 sec elicited by the voltage protocol shown.

Table 2. Properties of T84 cells recorded in extracellular Hanks solution

Resting potential	(mV)	−31 ± 2	(54)
Input resistance	(MΩ)	84 ± 13	(37)
Tau_m	(msec)	4.5 ± 0.4	(11)
Membrane capacitance	(pF)	106 ± 15	(11)

Values are mean ± SE of the number of experiments given in parentheses.

and suggests that the membrane potential of T84 cells is dominated by Cl^- conductance.

The input resistance (R_i) and time constant (τ_m) of change in membrane potential were estimated by passing a 50 msec square current pulse of 0.5 nA amplitude. These values are also listed in Table 2. The membrane capacitance was calculated from R_i and τ_m values which gave a value of 106 pF. This value of membrane capacitance can be used to estimate the membrane surface area making the assumption that the specific capacitance is 1 μFcm^{-2}. The calculated surface area in this case is calculated to equal 106×10^{-6} cm^2. This corresponds to a diameter of 100 μm assuming the cell to be a perfect sphere. This calculated diameter is consistent with the size of the cells observed under the microscope, which were chosen by their large size to facilitate impalements.

Voltage-Clamp Measurements

Voltage-clamp experiments were carried out in normal Hanks solution to identify the basal currents present in

[1] Once the anionic currents had declined by about 70%, replacing Na^+ by N-methyl-D-glutamine in the same low Cl^- medium shifted the reversal potential towards −40 mV (*results not shown*). This would suggest a small contribution from a cationic conductance selective for K^+ and Na^+ but rejecting the organic cation, which is most evident in the absence of Cl^- currents. Cationic conductances have also been reported in these cells by others (Devor & Duffey, 1992).

nonstimulated T84 cells. Cells were clamped at a holding potential of −40 mV and their membrane currents recorded at potentials of between −100 and 100 mV. The kinetic appearance of the currents recorded with this type of approach was variable from cell to cell. Three main apparent kinetics could be distinguished: currents that decayed during the voltage pulse at the most depolarized potentials, currents showing activation in depolarized pulses and apparent decay at hyperpolarization and currents that appeared to be time independent. Combinations of these apparent kinetic patterns could also be seen in many cases. The characteristics of these currents as well as their selectivity are discussed below. Regardless of the kinetics of the currents observed, they remained stable even during long recording times (up to 45 min).

Currents Showing Decay at Depolarizing Voltages

Figure 3*A* shows a family of currents (NaCl family) elicited by 600 msec voltage pulses from a holding potential of −40 mV. Large, outwardly rectifying currents were observed which, at the most depolarizing potentials, showed a decline during the course of the voltage pulse. The current-voltage relation for this experiment is shown in Fig. 3*B* (measurements were taken 6 msec after the onset of the pulse). The zero-current voltage was around −25 mV. Ion replacement experiments were conducted to ascertain the identity of the charge carrier involved in the decaying currents. When the extracellular Cl^- was replaced by gluconate, a strong inhibition of outward currents took place (Na-gluconate family). Figure 3*B* shows the corresponding current-voltage relation for the traces in *A*. Cl^- replacement instantaneously decreased outward currents, displaced the reversal potential toward 0 mV and increased inward currents. Assuming an intracellular Cl^- concentration of 30 mM, a permeability ratio $P_{gluconate}/P_{Cl}$ of 0.28 was obtained. The shape of the current-voltage relation changed from outwardly rectifying to slight inward rectification. Increasing extracellular K^+ to 50 mM (substituting Na^+) had no marked effect on the currents. This experiment suggests that the main charge carrier in the cell is Cl^- with little contribution from K^+. As the time after solution change was short (<1 min), it would be reasonable to assume that the cell had not yet been depleted of Cl^-. Hence, the increased inward current could be the result of Cl^- efflux under an increased driving force due to extracellular Cl^- removal. Experiments exploring the effect of prolonged superfusion with a low Cl^- solution on the decaying currents showed that after 10 min superfusion with gluconate-rich solution, a marked reduction in the size of both inward and outward currents occurred and the reversal potential shifted to around 0 mV (*result not shown*). This would suggest that after a longer period in a low Cl^- solution the cell had become depleted of Cl^-, and for this reason inward current was also greatly reduced.

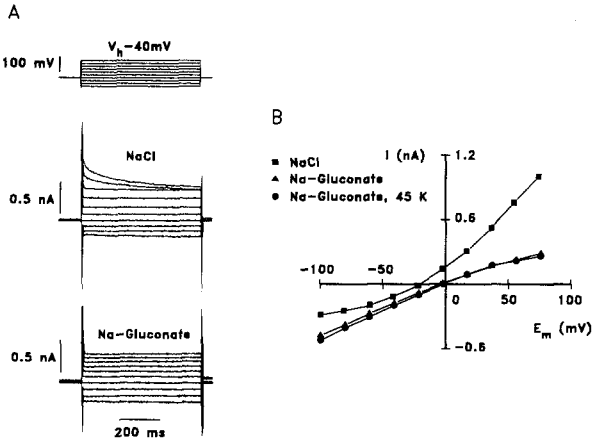

Fig. 3. Effect of Cl^- replacement on the decaying current of a T84 cell recorded with SEVC. (*A*) Families of currents elicited by voltage steps from a holding potential of −40 mV in a cell bathed in Hanks solution and 1 min after replacement of Cl^- by gluconate. (*B*) Corresponding current-voltage relations measured 6 msec after the onset of the pulse. A third set of data (circles) was obtained from the same cell after replacement of 40 mM Na^+ for 40 mM K^+ (total K^+ = 45 mM).

As to the kinetics of the decaying currents, it is noticeable that during depolarizing pulses a decay in currents took place during the voltage pulse. As discussed above for the patch-clamp whole-cell recordings, the kinetics of the current could be explained by a transient activation of previously silent channels or by closure of channels already active at the holding potential. The time to reach the peak should be discernible if this peculiar kinetics were the consequence of depolarization-dependent activation of channels silent at the holding potential. Figure 4*A* shows a family of currents acquired at high time resolution which shows that peak current was reached without any appreciable delay once the new potential was established. In Fig. 4*C* this point is made clearer by plotting the ratio of the steady-state to the maximum steady-state chord conductance against the membrane potential (inverted triangles), which indicates that depolarization produced a decrease in conductance. Examination of the effect of the holding potential on the current elicited by a depolarized voltage also indicated that closure of channels must occur during depolarization. Figure 4*B* shows the current elicited by a pulse to 100 mV after holding the membrane for 400 msec at voltages from −60 to 80 mV. The steady-state current was independent of the holding potential, but the instantaneous current declined as the prepulse was made more positive. In Fig. 4*C* this is quantified by plotting peak over the maximum peak current against

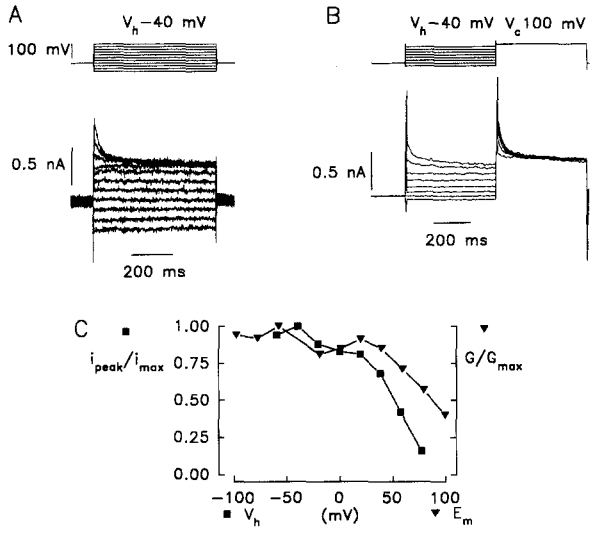

Fig. 4. Effect of holding potential on the decaying current. (*A*) Family of currents in response to voltage steps from a holding potential of −40 mV. The traces were acquired at 2,400 samples per second. (*B*) Family of currents elicited by a 100-mV voltage step after prepulses of between −60 and 80 mV. (*C*) Values of steady-state chord conductance (from *A*), relative to that measured at −60 mV, are plotted as a function of the voltage of the step (inverted triangles). A similar plot for the peak current from *B* for a given voltage, relative to that measured after a −60 mV prepulse, is also shown.

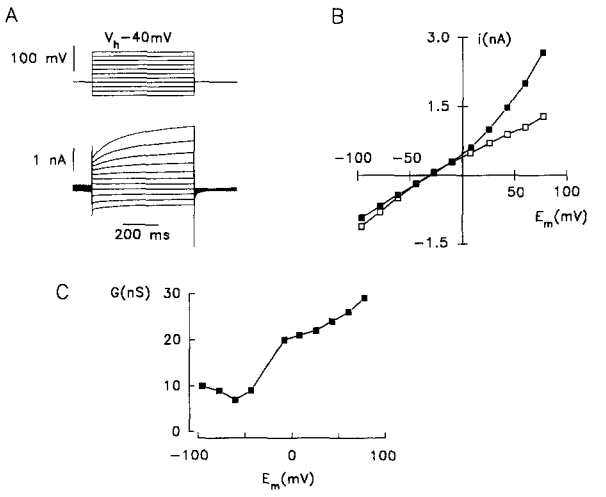

Fig. 5. Current recording showing depolarization-activated currents measured by the SEVC approach in a T84 cell. (*A*) Family of currents elicited by voltage steps from a holding potential of −40 mV. (*B*) Current-voltage relation measured 6 msec after the onset of the pulse (open squares) or at the steady-state (filled squares). (*C*) Values of steady-state chord conductance *vs.* membrane potential.

prepulse potential. The decrease in this ratio also indicates that active channels must close at depolarized potentials. It is also interesting that cells showing the depolarization-induced decay in current often showed a slow activation when pulsing to hyperpolarized potentials. This was most clear in experiments (*not shown*) where a variable prepulse was given before a pulse to a negative potential, during which activation was only discernible after depolarizing prepulses had been imposed.

Depolarization-activated Currents

A kinetically distinct current recorded in an unstimulated T84 cell is seen in Fig. 5*A* when pulsing the voltage between −100 and 80 mV. Here, a clear increase in current during depolarizing voltage pulses is evident, accompanied by a decrease in current at hyperpolarizing potentials. The corresponding current-voltage relations for instantaneous or steady-state currents are shown in Fig. 5*B*. Instantaneous currents were larger than those at steady-state for negative potentials while the contrary was true for positive potentials. The reversal potential was about −35 mV for both current-voltage relations. Figure 5*C* shows the steady-state conductance as a function of the membrane potential. A clear increase in conductance occurred at depolarizing potentials.

The nature of the ion(s) acting as charge carriers for the depolarization-activated currents was explored in ion replacement experiments. Figure 6*A* shows that rapid extracellular Cl^- removal (gluconate substitution) markedly reduced outward currents, slightly increased inward currents and displaced the reversal potential towards positive values. Also, the outward rectification disappeared. This is consistent with Cl^- selectivity in a situation where the cell is not depleted of Cl^- (assuming an intracellular Cl^- concentration of 30 mM, the calculated $P_{gluconate}/P_{Cl}$ was 0.23). With a longer exposure (10 min, as opposed to 45 sec) to low extracellular Cl^-, a much larger inhibition of the depolarization-activated current took place, consistent with intracellular Cl^- depletion. The kinetics of the currents illustrated in Figs. 5 and 6 is consistent with channels which open with depolarization and close at negative potentials. This idea was confirmed by the tail current protocol experiment illustrated in Fig. 7. Main voltage pulses given after a 100-mV prepulse produced inward relaxation or outward relaxations depending on the voltage of the main pulse. Figure 7*B* shows the zero-time extrapolated tail currents, which reversed at around −20 mV and leveled off at positive voltages. The rate of relaxation was also strongly voltage dependent; Figure 7*C* shows the time constants, derived from exponential fits of the tail currents, as a function of the potential. The rate of inactivation was markedly increased at hyperpolarized

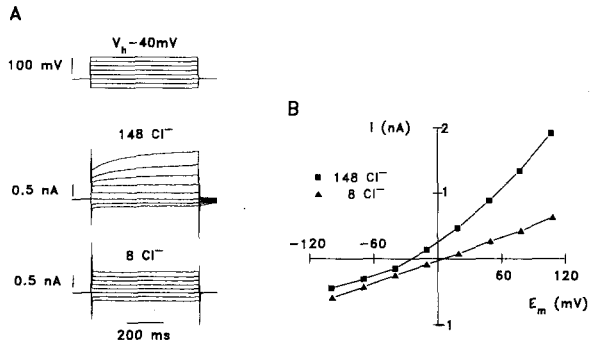

Fig. 6. Effect of Cl^- replacement on the depolarization-activated current recorded in a T84 cell. (*A*) Families of currents elicited by voltage steps from −40 mV in a cell bathed in Hanks and then 45 sec after removal of all but 8 mM Cl^- from the bathing solution. (*B*) Corresponding current-voltage relations.

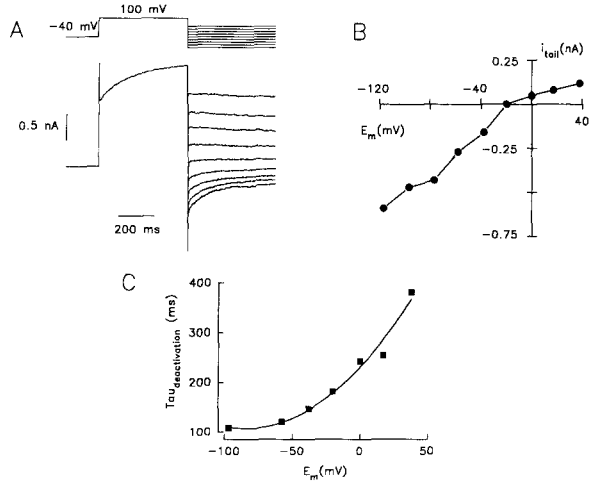

Fig. 7. Tail currents of the depolarization-activated currents. (*A*) Examples of tail currents obtained by stepping from a holding potential of −40 to 100 mV and then to potentials between −120 and 40 mV. Tail currents were fitted single exponential functions. The zero-time amplitudes of the tail currents are plotted as a function of the membrane potential in *B*. (*C*) Rate constants for deactivation are shown as a function of the membrane potential.

potentials, suggesting that the channels underlying these Cl^- currents are voltage activated.

Time-Independent Currents

A third type of current, rarely seen in isolation from the other kinetically distinguishable currents and characterized by its time independence, is shown in Fig. 8*A* (family 148 Cl^-). Voltage-clamp recordings are shown in *A* for a cell bathed in Hanks and pulsed between −80 and 80 mV. The voltage-clamp protocol produced

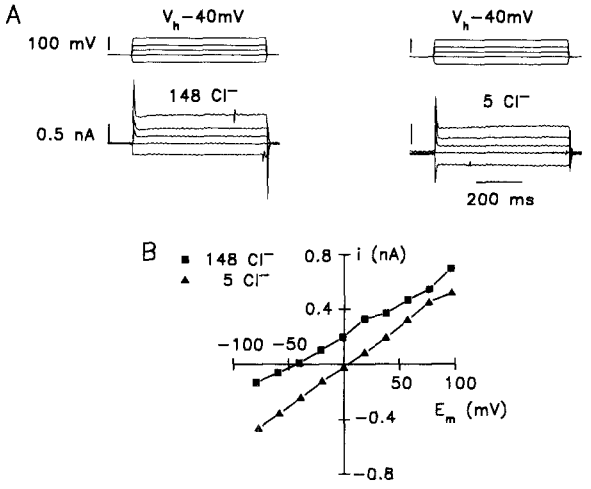

Fig. 8. Effect of Cl^- removal on the time-independent current of T84 cells. (*A*) Currents recorded in Hanks and 1 min after replacement of all but 5 mM extracellular Cl^- by gluconate. (*B*) Corresponding current-voltage relations.

time independent currents showing very slight outward rectification, if anything. This outward rectification could be due to the differences in the chloride concentration between the cell interior and the bathing solution. Cl^- appeared to be the charge carrier for the time-independent currents as replacement of most of the extracellular Cl^- by gluconate (family 5 Cl^-) reduced time-independent outward currents and shifted the reversal potential towards positive potentials (Fig. 8*B;* the calculated $P_{gluconate}/P_{Cl}$ was 0.13).

Cell Variability in Current Kinetics

The reason for the cell-to-cell variability in current patterns observed during voltage-clamp experiments in T84 cells is not clear. A possible explanation is that an artifact caused by microelectrode impalement could be the source of this variability. One possible consequence of artifactual impalement would be leakage of Ca^{2+} into the cell. To test this possibility, experiments were conducted by removing Ca^{2+} from the extracellular medium. Examination of a large number of experiments carried out in Ca^{2+}-containing medium revealed that 30% (12/40) of the voltage-clamped cells exhibited the decaying current, 52% (21/40) showed the slow-activating current and 18% (7/40) were of mixed kinetics or time independent. Of eight cells bathed in a Ca^{2+}-free solution from before the impalement, four showed the decaying current and four the slowly activating current. Consequently, it is unlikely that differential Ca^{2+} leakage into the cells might be the cause of the heterogeneity in current kinetic pattern.

Muscarinic Activation of a K^+ Conductance

To study this receptor-mediated response, the cells under study were challenged with a bathing solution containing 100 μM carbachol (Fig. 9). Figure 9*A* shows a family of membrane currents elicited in a cell bathed in Hanks solution, and 10 sec after the addition of 100 μM carbachol (CCh) to the bathing solution (*B*). The addition of CCh determined an increase of the outward currents (mainly the steady-state currents). This increase of the outward currents was associated with a hyperpolarization of about 20 mV (from −31 to −50 mV, Fig. 9*D*). The *I-V* relationship presented in *D* also shows the current measurements obtained 20 sec after the addition of CCh (open triangles), which were not different to the values measured before the agonist addition (squares), reflecting the transient nature of the CCh effect, already reported by others (Devor et al., 1990; Duffey & Devor, 1990). Figure 9*C* shows the current traces obtained by subtracting the control currents (Hanks) from currents seen in the presence of CCh. This yielded currents which had a zero-current potential of −82 mV. This potential is close to E_K, calculated from published intracellular K^+ concentrations (Mandel et al., 1986), suggesting that this current could be the consequence of K^+ channels activated by CCh.

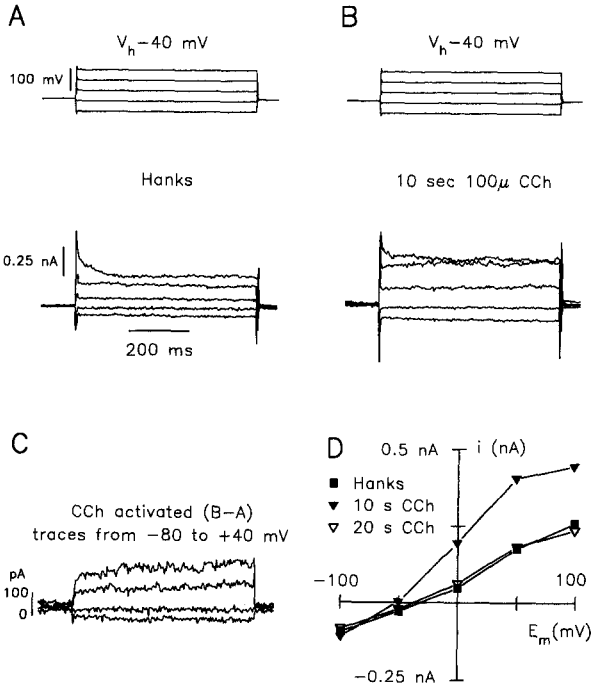

Fig. 9. Effect of CCh (100 μM) upon ion currents in a T84 cell measured by the SEVC approach. (*A*) Voltage-clamp records taken in control Hanks and (*B*) after bathing the cell for 10 sec in 100 μM CCh. (*C*) Traces obtained by subtracting currents in normal Hanks from those obtained in CCh. (*D*) Current-voltage relations for traces in Hanks (■), 10 sec in CCh (▼) and 20 sec in CCh (▽).

Discussion

Our present experiments using the patch-clamp technique and the single-electrode voltage-clamp technique to measure whole-cell currents in T84 cells show that Cl^- channels are active at rest and dominate the membrane potential. That most of the current observed in dialyzed cells is carried by Cl^- was confirmed by extracellular Cl^- removal, which markedly reduced outward currents, and by intracellular Cl^- removal, that greatly reduced inward currents. Although currents were initially large, they gradually decreased in magnitude during an experiment until they became negligible. In amphibian enterocytes, Cl^- and K^+ currents normally seen in nondialyzed cells are absent when studied by the patch-clamp whole-cell method (Sheppard et al., 1991; Valverde et al., 1991*b*). This has been interpreted to be due to the so-called washout of currents, which is assumed to occur through loss of some cytoplasmic component essential for the activity of the channels. We presume that this effect accounts for the gradual loss of currents seen here and for their virtual absence in unstimulated T84 cells reported before (Cliff & Frizzell, 1990; Devor et al., 1990). That this is a likely explanation has also been pointed out by Chan, Goldstein and Nelson (1992). These authors, using the perforated patch-clamp method (Horn & Marty, 1991), showed that airway epithelial cells presented a basal Cl^- conductance that disappeared after prolonged dialysis. The use of an intracellular microelectrode voltage-clamp technique, that avoids intracellular dialysis, has confirmed this hypothesis.

Single-electrode voltage-clamp experiments revealed three types of current patterns. They were characterized by their voltage and time dependence: a current active at the onset of depolarizing pulses but decaying markedly during the course of the voltage pulse; a current showing slow activation during depolarizing pulses and inactivation at hyperpolarizing pulses; and a current that was time independent. All these currents appeared to be carried by Cl^-, as revealed by ionic replacement experiments, and we shall refer to them as $I_{Cl(dec)}$, $I_{Cl(slow)}$ and $I_{Cl(t\text{-}i)}$, respectively, for the sake of brevity. Prolonged washing of cells in Cl^--free medium invariably reduced the currents to linear currents with a reversal point around 0 mV. This suggests that the electrochemical gradient for Cl^- is largely responsible for setting E_m in nonstimulated T84 cells, a contention that is supported by the closeness of the E_m value measured here with microelectrodes and the equilibrium potential for Cl^- deduced from published values for intracellular Cl^- concentration.

It is interesting to consider the transepithelial Cl^- transport data available for T84 cells in light of our ob-

servations. Under resting conditions, T84 monolayers do not effect net transepithelial transport of Cl^-. When stimulated with vasoactive intestinal peptide (VIP) or carbachol, net basal to apical Cl^- flux can be observed (Dharmsathaphorn & Pandol, 1986; Mandel et al., 1986). VIP stimulation, which raises the cellular levels of cAMP, appears to stimulate a sustained Cl^- secretion by activating apical Cl^- channels and basolateral K^+ channels. Carbachol, which raises intracellular Ca^{2+}, stimulates Cl^- secretion transiently by stimulating K^+ channels without a discernible effect on Cl^- conductance (Dharmsathaphorn & Pandol, 1986), although more recent work has shown that CCh also induces a Cl^- conductance in partially dialyzed T84 cells (Devor & Duffey, 1992). The conclusion gained from the transport studies was that there must be Cl^- channels in T84 cells that are active at rest, stimulation of K^+ conductance by carbachol would simply allow for cell hyperpolarization and efflux of Cl^- through tonically active channels. A similar conclusion was reached by Anderson and Welsh (1991) to explain the Ca^{2+}-dependent Cl^- secretion in T84 cells, pointing to the possibility of apical Cl^- channels open in the basal state. This view is upheld by our findings of large Cl^- conductance active at rest and a coincidence between E_m and E_{Cl}. In addition, the lack of dependence of the currents on K^+ concentration also argues for a low conductance to this cation which might then be rate-limiting to Cl^- efflux.

Muscarinic activation of Cl^- secretion has also been reported in the small intestinal crypts of the guinea-pig (Walters et al., 1992) and the mouse (Valverde et al., 1993*b*). The CCh effect on the guinea-pig crypt membrane potential is consistent with the activation of a K^+ conductance, as the agonist induced a hyperpolarization of about 15 mV (Walters & Sepúlveda, 1991; Walters et al., 1992). A similar effect was observed for the isolated colonic crypts of the rat (Bohme, Diener & Rummel, 1991). These authors, using the perforated patch-clamp technique, showed that the addition of CCh is associated with an increase in the outward currents and a shift of the zero-current level towards more negative values. This is similar to the results we have obtained with T84 cells in the present work (Fig. 9) and to previously published results obtained using the perforated-patch recording technique (Devor & Duffey, 1992). It is then possible that, as proposed for T84 cells, in colonic epithelium Ca^{2+}-dependent Cl^- secretion might occur through basally active Cl^- channels by activation of K^+ conductance.

The kinetically distinguishable currents observed in T84 cells using the SEVC approach are similar to Cl^- currents seen before in other epithelial cells but also in T84 cells after stimulation (for review, *see* Anderson et al., 1992). Our own results obtained using the whole-cell recording mode of the patch-clamp technique have shown that the different kinetic current patterns can be obtained depending on the nature of the stimulus in individual T84 cells and have suggested that they are the consequence of the activity of separate channels (Valverde et al., 1993*a*). Similarities between present results and those previously published are discussed below.

$I_{Cl(dec)}$

This current is similar to that observed first in respiratory epithelial cells by McCann, Li and Welsh (1989) and by Schoppa et al. (1989). According to these workers, the currents can be activated via a cAMP-mediated mechanism and also by exposing cells to hypotonic medium. McCann et al. (1989) maintain that the single channel mediating this type of current corresponds to an outwardly rectifying Cl^- channel that was originally associated with Cl^- secretion. This association has not been confirmed by later work. More recently, the type of kinetic behavior described here for $I_{Cl(dec)}$ was found to be associated with Cl^- currents stimulated by hypotonicity in airway epithelial and T84 cells (Worrell et al., 1989; Solc & Wine, 1991; Wagner et al., 1991), in HeLa cells (Diaz et al., 1993) and in cells transfected with the human *MDR*1 gene (Gill et al., 1992; Valverde et al., 1992). This kinetic behavior was very different from Cl^- currents activated in the same cells by cAMP or Ca^{2+} pathways.

$I_{Cl(act)}$

This current shares the kinetic appearance of that stimulated by an increase of intracellular Ca^{2+} in rat exocrine pancreas (Randriamampita, Chanson & Trautmann, 1988). It is also very similar to that stimulated by addition of Ca^{2+} ionophore in whole-cell patch-clamp recordings of airway epithelial and T84 cells (Cliff & Frizzell, 1990; Anderson & Welsh, 1991; Wagner et al., 1991). In addition to the general kinetic appearance of these currents, their conductance properties, which show inward rectification in tail current protocols (*see* Fig. 7), is also reminiscent of the Ca^{2+}-activated current described by Randriamampita et al. (1988) and by Anderson and Welsh (1991).

$I_{Cl(t\text{-}i)}$

This type of current was not seen often in isolation. It is nevertheless clearly present in some SEVC experiments and also features in some whole-cell patch-clamp recordings (*see* Fig. 1). The time independence of $I_{Cl(t\text{-}i)}$ would suggest an equivalence with cAMP-stimulated Cl^- currents observed in airway epithelium (Wagner et al., 1991), T84 cells (Cliff & Frizzell, 1990;

Anderson & Welsh, 1991), Caco-2 cells (Bear & Reyes, 1992) and in different cells transfected with the CFTR gene (*for review, see* Welsh et al., 1992).

It is not known why these currents that can be activated by different maneuvers in T84 cells are present without requirement for any stimulation when the cells are not dialyzed intracellularly. This finding, however, has two important implications: it provides an explanation for the findings of Dharmsathaphorn and Pandol (1986) that stimulation of a basolateral K^+ conductance alone can produce Cl^- secretion; and it suggests that the resting E_m value is determined by E_{Cl} in the nonstimulated T84 cells, making activation of the K^+ channel a prerequisite for secretion.

Finally, the question of whether the kinetically distinct currents described here represent the activity of different channels or the expression of the same channels after different modes of activation cannot be answered with the results available. It is interesting though to note that at least two types of single Cl^--selective channels having marked differences in conductance and kinetics have already been described in detail in T84 cells (Tabcharani et al., 1990). It is therefore not surprising to encounter a heterogeneity in macroscopic Cl^- currents in these epithelial cells.

G.M.V. and M.A.V. were supported by AFRC (UK) LRG 111 and DGICYT (Spain), respectively. We are grateful to John O'Brien for culturing the cells, to John Dempster (University of Strathclyde, Glasgow, UK) for providing the analysis software, and to Geoff Warhurst (Hope Hospital, Salford, UK) for generously providing the initial batch of T84 cells.

References

Anderson, M.P., Sheppard, D.N., Berger, H.A., Welsh, M.J. 1992. Chloride channels in the apical membrane of normal and cystic fibrosis airway and intestinal epithelia. *Am. J. Physiol.* **263:**L1–L14

Anderson, M.P., Welsh, M.J. 1991. Calcium and cAMP activate different chloride channels in the apical membrane of normal and cystic fibrosis epithelia. *Proc. Natl. Acad. Sci. USA* **88:**6003–6007

Bear, C.E., Reyes, E.F. 1992. cAMP-activated chloride conductance in the colonic cell line, Caco-2. *Am. J. Physiol.* **262:**C251–C256

Bohme, M., Diener, M., Rummel, W. 1991. Ca^{2+}- and cyclic-AMP mediated secretory responses in isolated colonic crypts. *Pfluegers Arch.* **419:**144–151

Chan, H-C., Goldstein, J., Nelson, D.J. 1992. Alternate pathways for chloride conductance activation in normal and cystic fibrosis airway epithelial cells. *Am. J. Physiol.* **262:**C1273–C1283

Cliff, W.H., Frizzell, R.A. 1990. Separate Cl^- conductances activated by cAMP and Ca^{2+} in Cl^- secreting epithelial cells. *Proc. Natl. Acad. Sci. USA* **87:**4956–4960

Devor, D.C., Duffey, M.E. 1992. Carbachol induces K^+, Cl^-, and nonselective cation conductances in T84 cells: a perforated patch-clamp study. *Am. J. Physiol.* **263:**C780–C787

Devor, D.C., Simasko, S.M., Duffey, M.E. 1990. Carbachol induces oscillations of membrane potassium conductance in a colonic cell line, T84. *Am. J. Physiol.* **258:**C318–C326

Dharmsathaphorn, K., Pandol, S.J. 1986. Mechanism of chloride secretion induced by carbachol in a colonic epithelial cell line. *J. Clin. Invest.* **77:**348–354

Diaz, M., Valverde, M.A., Higgins, C.F., Rucareaunu, C., Sepúlveda, F.V. 1993. Volume-activated chloride channels in HeLa cells are blocked by verapamil and dideoxyforskolin. *Pfluegers Arch.* **422:**347–353

Duffey, M.E., Devor, D.C. 1990. Intracellular pH and membrane potassium conductance in rabbit distal colon. *Am. J. Physiol.* **258:**C336–C343

Finkel, A.S., Redman, S. 1984. Theory and operation of a single-microelectrode voltage clamp. *J. Neurosci. Meth.* **11:**101–127

Gill, D.R., Hyde, S.C., Higgins, C.F., Valverde, M.A., Mintenig, G.M., Sepúlveda, F.V. 1992. Separation of drug transport and chloride channel functions of the human multidrug resistance P-glycoprotein. *Cell* **71:**23–32

Horn, R., Marty, A. 1991. Muscarinic activation of ionic currents measured by a new whole-cell recording method. *J. Gen. Physiol.* **92:**145–149

Mandel, K.G., Dharmsathaphorn, K., McRoberts, J.A. 1986. Characterisation of a cyclic AMP activated Cl^- transport pathway in the apical membrane of a human colonic epithelial cell line. *J. Biol. Chem.* **261:**704–712

McCann, J.D., Li, M., Welsh, M.J. 1989. Identification and regulation of whole-cell chloride currents in airway epithelium. *J. Gen. Physiol.* **94:**1015–1036

Randriamampita, C., Chanson, M., Trautmann, A. 1988. Calcium and secretagogue-induced conductances in rat exocrine pancreas. *Pfluegers Arch.* **411:**53–57

Schoppa, N., Shorofsky, S.R., Jow, F., Nelson, D.J. 1989. Voltage-gated chloride currents in cultured canine tracheal epithelial cells. *J. Membrane Biol.* **108:**73–90

Sheppard, D.N., Valverde, M.A., Giraldez, F., Sepúlveda, F.V. 1991. Potassium currents of isolated *Necturus* enterocytes: a whole-cell patch-clamp study. *J. Physiol.* **433:**663–676

Solc, C.K., Wine, J.J. 1991. Swelling-induced and depolarization-induced Cl^- channels in normal and cystic fibrosis epithelial cells. *Am. J. Physiol.* **261:**C658–C674

Suzuki, S., Tachibana, M., Kaneko, A. 1990. Effects of glycine and GABA on isolated bipolar cells of the mouse retina. *J. Physiol.* **421:**645–662

Tabcharani, J.A., Low, W., Elie, D., Hanrahan, J.W. 1990. Low-conductance chloride channel activated by cAMP in the epithelial cell line T84. *FEBS Lett.* **270:**157–164

Valverde, M.A., Diaz, M., Sepúlveda, F.V., Gill, D.H., Hyde, S.C., Higgins, C.F. 1992. Volume-regulated chloride channels associated with the multidrug resistance P-glycoprotein. *Nature* **355:**830–833

Valverde, M.A., Mintenig, G.M., Sepúlveda, F.V. 1991*a*. Cl^- conductance determines the membrane potential of unstimulated intestinal epithelial T84 cells. *J. Physiol.* **438:**334P

Valverde, M.A., Mintenig, G.M., Sepúlveda, F.V. 1993*a*. Differential effects of tamoxifen and I- on three distinguishable chloride currents activated in T84 intestinal cells. *Pfluegers Arch.* **425:**552–554

Valverde, M.A., O'Brien, J.A., Sepúlveda, F.V., Ratcliff, R., Evans, M.J., Colledge, W.H. 1993*b*. Inactivation of the murine *cftr* gene abolishes cAMP-mediated but not Ca^{2+}-mediated secretagogue-induced volume decrease in small intestinal crypts. *Pfluegers Arch.* **425:**434–438

Valverde, M.A., Sheppard, D.N., Giraldez, F., Sepúlveda, F.V. 1991*b*. Two types of potassium currents seen in isolated *Necturus* enterocytes with the single-electrode voltage-clamp technique. *J. Physiol.* **433:**645–661

Wagner, J.A., Cozens, A.L., Schulman, H., Gruenert, D.C., Stryer, L.,

Gardner, P. 1991. Activation of chloride channels in normal and cystic fibrosis airway epithelial cells by multifunctional calcium/calmodulin-dependent protein kinase. *Nature* **349:**793–796

Walters, R.J., O'Brien, J.A., Valverde, M.A., Sepúlveda, F.V. 1992. Membrane conductance and cell volume changes evolved by VIP and carbachol in small intestinal crypts. *Pfluegers Arch.* **421:**598–605

Walters, R.J., Sepúlveda, F.V. 1991. A basolateral K^+ conductance modulated by carbachol dominates the membrane potential of small intestinal crypts. *Pfluegers Arch.* **419:**537–539

Welsh, M.J., Anderson, M.P., Rich, D.P., Berger, H.A., Denning, G.M., Ostedgaard, L.S., Sheppard, D.N., Cheng, S.H., Gregory, R.J., Smith, A.E. 1992. Cystic fibrosis transmembrane conductance regulator: A chloride channel with novel regulation. *Neuron* **8:**821–829

Wilson, W.A., Goldner, M.M. 1975. Voltage clamping with a single microelectrode. *J. Neurobiol.* **6:**411–422

Worrell, R.T., Butt, A.G., Cliff, W.H., Frizzell, R.A. 1989. A volume-sensitive chloride conductance in human colonic cell line T84. *Am. J. Physiol.* **256:**C1111–C1119